Reaction Chemistry & Engineering

Mechanism of tetralin conversion on zeolites for production of benzene derivatives

Journal:	*Reaction Chemistry & Engineering*
Manuscript ID	RE-ART-04-2020-000128.R1
Article Type:	Paper
Date Submitted by the Author:	12-May-2020
Complete List of Authors:	Nakajima, Kazuki; Tottori Daigaku, Center for Research on Green Sustainable Chemistry Suganuma, Satoshi; Tottori Daigaku, Center for Research on Green Sustainable Chemistry Tsuji, Etsushi; Tottori Daigaku, Department of Chemistry and Biotechnology, Graduate School of Engineering Katada, Naonobu; Tottori University, Department of Chemistry and Biotechnology, Graduate School of Engineering

Mechanism of tetralin conversion on zeolites for production of benzene derivatives

Kazuki Nakajima, Satoshi Suganuma,* Etsushi Tsuji, Naonobu Katada

Center for Research on Green Sustainable Chemistry, Tottori University, 4-101 Koyama-cho Minami, Tottori 680-8552, Japan

Phone: +81-857-31-5256; Fax: +81-857-31-5684; E-mail: suganuma@tottori-u.ac.jp

Keywords

Tetralin; benzene derivatives; zeolite; ring-opening; acidity

Abstract

Ring-opening of tetralin, which is produced by partial dehydrogenation of naphthalene, was catalyzed by various zeolites. Influences of acidity and textual property of the zeolites on activity and selectivity were studied in the reactions of not only tetralin but also butylbenzene and indane as the intermediate models in tetralin conversion. The *BEA zeolite exhibited higher conversion and selectivity of benzene and its derivatives (butylbenzene, toluene, xylenes and ethylbenzene) than the other framework type zeolites. The simultaneous cracking of butylbenzene principally produced benzene. The reaction rate in ring-opening of tetralin was considerably high on strong Brønsted acid sites in 12-ring of *BEA zeolite. The amount of Brønsted acid sites on *BEA zeolite increased the tetralin conversion but did not affect the selectivity of the products. In tetralin conversion MOR and FAU zeolites formed more methylindane and naphthalene as byproducts, respectively. Methylindane was produced on weak Brønsted acid sites through ring-contraction of tetralin, and naphthalene was formed on Lewis acid sites through dehydrogenation. The influences of the reaction conditions on the catalytic activity in tetralin conversion were also

investigated. The contact time increased the conversion, but hardly affect the selectivities of the products. The total pressure also improved the catalytic activity. The pressurized hydrogen decreased the selectivity of methylindane, while increased benzene and its derivatives. At 573 K the selectivities of benzene and its derivatives were high, but the reaction temperature increased the selectivity of the byproducts.

1. Introduction

Crude oil has been upgraded to available hydrocarbons by atmospheric and vacuum distillation followed by hydrogenation/hydrocracking or fluid catalytic cracking (FCC) of vacuum gas oil in petroleum refinery process (**Figure 1**) [1-3]. Benzene and its derivatives such as BTX (benzene, toluene and xylenes) and the other alkylbenzenes are essential resources of chemical intermediates and gasoline [4]. However, the conventional processes have many problems from a view of benzene derivatives production[5]. In hydrogenation/hydrocracking, alkanes (paraffins) are mainly produced via hydrogenation of polycyclic aromatic hydrocarbons followed by ring-opening and cracking of cycloalkanes. If complete hydrogenation of polycyclic aromatic hydrocarbons is desired, yield of monoaromatic hydrocarbons decreases, large amount of hydrogen is consumed, and undesired off-gas (<C2 alkanes) is formed [6]. Hydrogenation of aromatic hydrocarbon hardly proceeds in FCC, which produces smaller molecules by β-scission of C-C bond [7], leading generation of large amount of light cycle oil (LCO) including polycyclic aromatic hydrocarbons without alkyl groups [3,8], causing soot exhaust when it is used as a fuel [9,10]. Hence, a technology upgrading polycyclic aromatic hydrocarbons is necessary.

We have studied production and separation of alkanes with keeping the long chain lengths and aromatic compounds with removing completely the alkyl branches by dealkylation of alkyl polycyclic aromatic hydrocarbon in heavy oil over alumina-supported silica monolayer catalyst [11] (**Figure 2**). The long-chain alkanes can be utilized as diesel fuel and lubricant base oil [12], and the aromatics can be utilized as chemical feedstocks. However, it is difficult to utilize the polycyclic aromatic compounds such as naphthalene and phenanthrene for fuels nor chemicals, and therefore it is necessary to develop a way for efficient conversion of the polycyclic aromatic compounds to benzene derivatives through partial hydrogenation and then ring-opening (**Figure 2**) [13].

The conversion of polycyclic aromatic compounds in practical oil to benzene derivatives has been studied by several groups [14-16]. The industrial production of benzene derivatives from LCO has already operated in some oil refineries [17]. In this process, the feed enriched with aromatics was treated with hydrogenation/hydrocracking, and the catalytic reforming is applied to conversion of the products (cycloalkanes and alkanes) to form benzene derivatives through aromatization. High energy consumption and low yield of benzene derivatives are the problems to be overcome. In contrast, the formation of benzene derivatives through partial hydrogenation of naphthalene, as a main component in LCO, into tetralin and subsequent ring-opening has recently studied (**Figure 2**) [18-21]. For the former step, i.e., the partial hydrogenation of naphthalene, molybdenum-containing materials showed high catalytic activity and tetralin selectivity [21-25]. On the contrary, the conversion of tetralin into benzene derivatives, the latter step, has been known to be catalyzed by various zeolites [26-30], but the selectivity of benzene derivatives has been low.

Based on these backgrounds, we here study the reaction pathway and the influences of acidity and textural properties of zeolites on the catalytic activity and selectivity in tetralin conversion in hydrogen. A method of ammonia IRMS (infrared/mass spectroscopy) – TPD (temperature-programmed desorption) [31] is applied to show the the number, energy of ammonia desorption (index of acid strength) and type of Brønsted or Lewis acid sites on zeolites. In addition, catalytic activities of the zeolites were compared in the reactions of not only tetralin but also butylbenzene and indane to show influences of the acidity and textural properties of zeolites on reactivity in the reaction pathways. Furthermore, influences of the reaction conditions (contact time, hydrogen pressure and reaction temperature) were found to clarify the conditions suitable for the conversion of tetralin into benzene and its derivatives.

2. Experimental

2.1. Zeolite samples

Table 1 shows the zeolite catalysts applied in this study. The Na-form samples were transformed into NH_4-forms through ion-exchange in NH_4NO_3 aqueous solutions (NH_4/Na molar ratio: 10) at 353 K for 4 h and the following filtration, which were repeated 3 times. The thus obtained NH_4-form zeolites were dried at 383 K overnight. OSDA (organic structure-directing agent) on B28 was decomposed with heating at 773 K in air for 4 h, and H-form of B28 was obtained. H-form zeolites were applied as received.

2.2. Catalyst characterization

The nitrogen adsorption isotherm was measured at 77 K using a BELSORP-max equipment (Microtrac-BEL) after pretreatment at 573 K for 1 h under evacuation conditions. The micropore volume and the area of external surface including the walls of meso- and macropores was calculated by the *t*-plot method [32]. In addition, the volume of liquid nitrogen condensed at $P/P_0 \approx 0.005$ to fill the micropores was calculated as a reference of micropore volume by the following numerical expression Ex. (1).

$$\text{Condensed liquid nitrogen volume } [\mathrm{cm^3\ g^{-1}}] =$$

$$\frac{Amount\ of\ adsorbed\ N_2\ at\ P/P_0 = 0.005\ [\mathrm{mol\ g^{-1}}] \times Molar\ weight\ of\ N_2\ [28.01\ \mathrm{g\ mol^{-1}}]}{Density\ of\ liquid\ N_2\ at\ 77\ K\ [0.808\ g\ cm^{-3}]} \qquad \text{Ex. (1)}$$

Amount and strength of Brønsted and Lewis acid sites and sites were analyzed by an NH_3 IRMS-TPD method [31]. A self-supporting disc (1 cm diameter) was molded from the sample by compression, held in a set of metal rings and fixed in a cell of Microtrac-BEL IRMS-TPD analyzer. The sample was pretreated at 823 K for 1h in O_2 flow (34 μmol s^{-1}). After evacuation, the temperature was cooled to 343 K in vacuum. IR reference spectra as $N(T)$ were collected once at 1 K with heating the sample in a helium flow (68 μmol s^{-1}, 6 kPa) at 2 K min^{-1}. The ammonia was adsorbed under 13 kPa at 343 K and evacuated for 30 minutes. After keeping in a helium flow at 343 K for 3 hours, the sample was heated under the same conditions as well as before adsorption. At this time, IR spectra of adsorbed ammonia and MS response were measured. Difference spectra were calculated as $A(T)$ - $N(T)$. The ammonia TPD profile for each of Brønsted and Lewis acid site was analyzed according to our previous study [33]. The number of acid sites was calculated from the peak intensity of the TPD, and the distribution of enthalpy of ammonia desorption (so-called adsorption heat) was analyzed by the curve fitting method.

2.3. Catalytic reactions

The catalytic reactions were performed in a fixed-bed flow reactor (**Figure 3**). The catalyst (0.05-0.30 g) was placed in a stainless tube with inner diameter 4 mm and then pretreated at 823 K for 1 h in a flow of H_2 (134 mmol h^{-1}). The flow rate of reactants [tetralin, butylbenzene or indane (Tokyo Chemical Industry)] was 16.6 mmol h^{-1}, corresponding to W_{cat} / $F_{reactant}$ = 3-18 g h mol^{-1} at 523-823 K, whereas that of H_2 was 134 mmol h^{-1}. Total pressure in the reactor was kept at 1-4 MPa using a back-pressurized valve. The outlet effluents were trapped in a glass tube at 273 K and analyzed using a gas chromatograph (GC-2014, Shimadzu) with a flame ionization detector and a capillary column (InertCap1, 5.0 μm thickness in length 30 m and internal diameter 0.53 mm). The products were classified into benzene, TEX (toluene, ethylbenzene and xylenes), butylbenzene, methylindane, decalin and naphthalene. The untrapped gas products and the undetected products by the GC, such as deposited hydrocarbons on the catalysts, were defined as others. Conversion, yield, selectivity and turnover frequency (TOF) were calculated by the following equations.

$$\text{Conversion} = 1 - \frac{\text{Rate of reactant recovery } [\text{mol s}^{-1}]}{\text{Rate of reactant feed } [\text{mol s}^{-1}]}$$

$$\text{Yield} = \frac{\text{Rate of product formation } [\text{mol s}^{-1}]}{\text{Rate of reactant feed } [\text{mol s}^{-1}]}$$

$$\text{Selectivity} = \frac{\text{Yield}}{\text{Conversion}}$$

and

$$\text{Turnover frequency (TOF)} = \frac{\text{Flow rate of a reactant } [\text{mol h}^{-1}] \times \text{Conversion}}{\text{acid amount } [\text{mol kg}^{-1}] \times \text{A catalyst } [\text{kg}]}$$

3. Results

3.1 Acidity profiles and physical properties

A method of NH_3 IRMS-TPD determined the acidity of the zeolites [34]. **Figure S1-S3** show difference IR spectra obtained on the zeolites during the TPD experiments. A sharp band at ca. 1450 cm^{-1} was assigned to bending (ν_4) vibration of NH_4^+ adsorbed on Brønsted acid sites (NH_4^+ (BAS)). Also, a small peak at 1250-1330 cm^{-1} was assigned to bending (δ_s) vibration of NH_3 adsorbed on Lewis acid sites (NH_3 (LAS)). **Figure S4** shows TPD profiles of ammonia desorbed from the acid sites. MS-TPD indicates the profile of NH_3 desorption evaluated with mass spectroscopy. The TPD profiles were calculated from the IR-TPD of ca. 1450 cm^{-1}-band (ν_4, NH_4^+ (BAS)) and

1250-1330 cm^{-1}-band (δ_s, NH_3 (LAS)), respectively. **Table 2** shows the amounts of Brønsted acid sites (BAS) and Lewis acid sites (LAS) on the zeolite samples. The amounts of BAS on M15, Z22 and B28 were almost the same. Y5 possessed more BAS than the other zeolites. LAS was contained on the only Y5. The amount of BAS on B28 was approximately same to the aluminum content, unlike the other *BEA type zeolites. The order of BAS amount was B28 > > B25 > B150 > B500. Enthalpy (ΔH) of ammonia desorption from the BAS on catalysts is indicated as a index of Brønsted acid strength [31]. The order of the acid strength was M15 > Z22 > B28 > Y5. Bands at 3585 and 3616 cm^{-1} were assigned to the strong and weak BAS on M15 contained in 8-ring and 12-ring, respectively, as previously found (**Figure S3**) [35]. They were in the ratio of 2:1 (strong/weak). The acid strength of *BEA zeolites with different aluminum contents was similar. The micropore volume and external surface area are shown in **Table 2**. The micropore volumes of M15, Z22, and Y5 were similar to the values of the same framework types [36], while those of *BEA type zeolites applied in this study were larger than the literature values [37]. The external surface area is here showing the area of surfaces except the micropore wall and hence includes the surfaces of mesopore and macropore. B25 and B150 possessed larger external surface areas than the others.

3.2 Influence of zeolite framework types on catalytic activity

Figure S5 shows tetralin conversion and the product selectivities as a function of time on stream in the reaction of tetralin over the zeolites with different frameworks, which possessed approximately same quantity of BAS. The conversion on all the zeolites was gradually decreased with the time on stream, and showed an almost plateau over 2 h. The product selectivity also indicated a plateau over 2 h. The average conversion and selectivity between 3-5 h are reported. The activity on the various zeolites was compared on the basis of turnover frequency (TOF). **Figure 4** shows TOF and the product selectivity on the catalysts. TOF on B28 showed considerably higher than the other zeolites. In this reaction, the desired products are benzene and its derivatives, such as TEX (toluene, ethylbenzene and xylenes) and butylbenzene. The whole selectivities of benzene and its derivatives on B28 and Z22 was exhibited higher than that on M15 and Y5. In detail, B28 and Z22 showed higher selectivities into butylbenzene and TEX, than the other catalysts, respectively. M15 preferably formed methylindane as a byproduct. The reaction rates of dehydrogenation into naphthalene and hydrogenation into decalin on Y5 were higher than those on the other catalysts. The other products undetected by the present method are considered to be carbonaceous deposit on the catalysts and gaseous compounds such as C1-4 hydrocarbons, which were produced by cracking of alkyl groups. However, the flow rate of tetralin (1.1 g h^{-1}) was considerably more than the amount of catalyst (0.05-0.30 g). Therefore, most of the missing carbon was not deposited on the catalyst, but converted into C1-4 gases.

The reactions of butylbenzene and indane as models of the intermediates in tetralin conversion over the zeolites with different frameworks were performed to comprehend the reaction pathways. **Figure 5** displays the conversion and selectivity in the reactions of butylbenzene. The conversion on B28 was considerably higher than the other zeolites, and it is thus difficult to directly compare the product selectivity on B28 than the other zeolites. Benzene was formed by cracking of butylbenzene, and the benzene selectivity was M15 > Y5 > Z22. Methylindane was formed by cyclization of butylbenzene, and the methylindane selectivity was Y5 > M15 > Z22. The selectivity of undetectable products on Z22 was higher than those on the other catalysts. **Figure 6** shows the conversion and selectivity in the reaction of indane. All the catalysts showed very low conversion of indane in this set of reaction conditions. Small amounts of benzene and TEX were produced on B28.

The influence of Brønsted acid amount on *BEA type zeolite was explored in the tetralin conversion (**Figure 7**). Increase of the Brønsted acid amount increased the tetralin conversion, while it hardly affected the selectivity. B28 exhibited the highest catalytic activity among the *BEA type samples.

3.3 Influence of reaction conditions on catalytic activity

The influence of reaction conditions such as contact time, total pressure and reaction temperature on the catalytic activity of B28 was investigated in tetralin conversion. **Figure 8** shows the influence of contact time (W/F) on the tetralin conversion and selectivity at 623 K under 4 MPa of the total pressure. The feed rates of tetralin and hydrogen were constant, while the catalyst loading was varied. Increase of the contact time increased the conversion. The selectivity was methylindane > benzene > naphthalene > butylbenzene > TEX >> decalin, as already stated. The selectivities of methylindane and benzene decreased with increasing the contact time, whereas the selectivity of TEX slightly increased. **Figure 9** demonstrates the influence of total pressure on the catalytic activity at 623 K with 12 g h mol^{-1} of the contact time. The conversion was increased with the pressure elevation. The selectivity of methylindane, the main product, decreased, while the whole selectivity of benzene and its derivatives (butylbenzene and TEX) increased. The selectivity of naphthalene slightly decreased. **Figure 10** shows the influence of reaction temperature on the catalytic activity under 4 MPa of the total pressure with 12 g h mol^{-1} of the contact time. The conversion increased up to 80 % with elevation of the reaction temperature. The selectivities of benzene and butylbenzene exhibited maximum values at 573 K, but gradually decreased above 573 K. The selectivity of methylindane increased up to 673 K, and then decreased. TEX and naphthalene gradually increased up to 823 K.

4. Discussion

The influence of zeolite framework types on the catalytic activity in tetralin conversion is here discussed. The activities of the zeolites were compared on the basis of TOF. B28 showed considerably higher activity for the ring-opening and cracking of tetralin into butylbenzene, benzene and TEX than M15, Z22 and Y5. The amount of BAS on B28 and M15 was smaller than Z22 and Y5. Therefore, it is considered that the observed higher activity was ascribed to the *BEA type framework. The essential factors on the catalytic activity should be the strong BAS and accessibility of tetralin as the reactant. It is believed that tetralin (molecular dimension: 0.74 nm) was difficult to diffuse in 10-ring with 0.5-0.6 nm of the diameter on the MFI zeolite and 8-ring with 0.57 nm × 0.26 nm of the size on the MOR zeolite, in which the strong BAS were located preferentially but not in the 12-ring (0.70 nm × 0.65 nm) [35]. These should be reasons for the low activity of MFI and MOR. The *BEA zeolite possesses strong BAS in 12-ring (0.56 nm × 0.56 nm and 0.77 nm × 0.66 nm), and the catalytic activity was superior as above. Concerning the selectivity, B28 and Z22 formed larger extent of benzene and its derivatives than the other catalysts, whereas the main products on M15 and Y5 were methylindane and naphthalene, respectively. The high selectivity into benzene and its derivatives was ascribable to the strong Brønsted acid sites in 10- or 12-rings on *BEA and MFI. A distinct selectivity into naphthalene and decalin on Y5 (FAU) can be related with high catalytic activity for the hydrogenation / dehydrogenation through addition / abstraction of hydride species by LAS.

The results of reaction started from butylbenzene lead us total understanding of influences of zeolite framework types on the selectivities in tetralin conversion. The considerably high conversion of butylbenzene mainly into benzene and TEX on B28 indicates that the strong BAS in 12-ring on *BEA catalyzed the conversion of butylbenzene as well as tetralin, and cracking of butylbenzene into benzene and TEX mainly proceeded on the BAS. M15 (MOR with strong BAS in 8-ring) and Z22 (MFI with strong BAS in 10-ring) formed benzene, probably catalyzed by the BAS. The conversion on M15 and Z22 was low, presumably because the strong BAS were located in relatively small pores on these zeolites. The dehydrogenative cyclization of butylbenzene ($C_{10}H_{14}$) into methylindane ($C_{10}H_{12}$) was found on M15, Y5, and B28, and the selectivity was highest on Y5 (FAU), which contained a large amount of LAS. The cyclization involving the dehydrogenation step, like hydrogenation / dehydrogenation of tetralin as above, was speculated to be fast on LAS compared to BAS. The formation of methylindane was also considerable on M15. MOR had the strong BAS only in 8-ring, and the cyclization of butylbenzene into methylindane should require a wide pore compared to the cracking of butylbenzene into benzene. It implies that the weak BAS in 12-ring of MOR catalyzed the cyclization of butylbenzene into methylindane. On the other hand, indane was hardly reacted in the employed conditions (at 623 K under 4.0 MPa of total pressure) on M15, Z22, Y5, and B28. It suggests that indane framework was stable in these conditions, and there was a side reaction pathway from butylbenzene into methylindane as a goal, in addition to the desired reaction pathway from butylbenzene into benzene and TEX.

To take the above discussion into account, the reaction pathways are drawn as **Figure 11**. Strong BAS such as those on *BEA and MFI catalyzed ring-opening of tetralin into butylbenzene through an ipso addition of a hydrogen atom on tetralin and then a hydrogen-transfer from other hydrogen or hydrocarbon molecules [28]. Subsequently, butylbenzene was cracked into benzene and TEX on the BAS, while a part of butylbenzene was converted into methylindane through intramolecular addition. The ring-contraction of tetralin into methylindane is speculated to proceed even on weak BAS such as those in 12-ring on M15. In addition, a C-C bond between the benzene ring and methylene part in tetralin was dissociated, and then methylindane may be produced by intramolecular addition [28]. All of above reactions were inhibited by LAS on Y5, because it catalyzed the dehydrogenation of tetralin through abstraction of hydride species and then disproportionation, and finally formed naphthalene [28]. For the desired reaction, namely, conversion of tetralin into benzene and TEX, the strong BAS in 12-ring thus contributed, and therefore the *BEA type zeolite showed high activity and selectivity. The activity was increased with increasing the amount of BAS on *BEA zeolites with keeping the selectivity.

The influence of reaction conditions on the reaction rate and selectivity in tetralin conversion are here summarized. The selectivity of benzene, butylbenzene and naphthalene was not varied, while methylindane decreased and TEX slightly increased with increase of the contact time (W/F). It is speculated that a part of methylindane was converted into a set of TEX and small hydrocarbons by subsequent cracking of alkyl group.

Increase of the total pressure, in which most pressure was that of hydrogen, gained the conversion of tetralin. The selectivities of methylindane and naphthalene decreased, while benzene and its derivatives increased with increasing the total pressure. The high hydrogen pressure probably made the addition of hydrogen atoms on tetralin readily, and therefore the whole selectivity of butylbenzene, benzene and TEX were increased. Elevation of the reaction temperature increased the conversion, as naturally observed. The selectivities of butylbenzene and benzene were high at low temperature, whereas methylindane became the main product at 673 K. The addition of hydrogen to tetralin is suggested to be difficult at the high temperature like 623 K. It is speculated that butylbenzene was converted into benzene and TEX through the dealkylation over 523 K and cracking of the alkyl group over 623 K, respectively. In addition, it is revealed that TEX was not converted into benzene at even high temperature. Methylindane could not be converted at 623 K, but was shown to be cracked into TEX but benzene at the further high temperatures. The higher temperature realized dehydrogenation of tetralin into naphthalene, which may be non-catalytically and irrelevant to the Brønsted acid sites on the catalysts. The selectivity was thus strongly affected by the hydrogen pressure and reaction temperature.

5. Conclusions

*BEA type zeolite exhibited higher tetralin conversion than MFI, MOR and FAU zeolites. The selectivity of benzene and its derivatives, especially butylbenzene and benzene, was superior on *BEA and MFI zeolites. It is speculated that strong Brønsted acid sites in 12-ring on *BEA zeolite produced the benzene and its derivatives by ring-opening of tetralin and cracking of butylbenzene. Although MFI zeolite had Brønsted acid sites, the activity was low, presumably because the micropore size (10-ring) was smaller than molecular size of tetralin. MOR zeolite showed high selectivity of methylindane. The weak Brønsted acid sites such as those in 12-ring on MOR are speculated to catalyze the ring-contraction of tetralin into methylindane, On the other hand, due to the presence of large amount of Lewis acid sites, FAU zeolite formed large amount of naphthalene with small amount of decalin through dehydrogenation / hydrogenation of tetralin. The activity of *BEA zeolites increased with increasing the Brønsted acid sites with keeping the selectivity. On the *BEA zeolite, the contact time increased the tetralin conversion, whereas the selectivity of benzene and its derivatives was not largely affected. Increasing the hydrogen pressure increased the tetralin conversion and the selectivity of benzene and its derivatives. The high hydrogen pressure is speculated to promote the addition of hydrogen on tetralin to form butylbenzene. At 573 K, the selectivity of benzene and its derivatives was high. However, elevating the reaction temperature increased the selectivity of methylindane and naphthalene. High selectivity of benzene and its derivatives, especially butylbenzene, was observed under high hydrogen pressure and low reaction temperature.

Conflicts of interest

There are no conflicts to declare.

Acknowledgements

A part of this work was carried out as a part of Projects for technological development trusted by Ministry of Economy, Trade and Industry, Japan to Japan Petroleum Energy Center. The other part was supported by JSPS KAKENHI Grant Number 16H04568. Also, this study was partly supported by JST CREST Grant Number JPMJCR17P1, Japan.

1 **References**

1 R. Sahu, B.J. Song, J.S. Im, Y.P. Jeon, C.W. Lee, *J. Ind. Eng. Chem.*, 2015, **27**, 12.

2 S. Mehla, S. Kukade, P. Kumar, P.V.C. Rao, G. Sriganesh, R. Ravishankar, *Fuel.* 2019, **242**, 487.

3 E.T.C. Vogt, B.M. Weckhuysen, *Chem. Soc. Rev.*, 2015, **44**, 7342.

4 A.M. Niziolek, O. Onel, Y.A. Guzman, C.A. Floudas, *Energy Fuels.*, 2016, **30**, 4970.

5 C. Marcilly, *J. Catal.*, 2003, **216**, 47.

6 M.S. Rana, V. Sámano, J. Ancheyta, J.A.I. Diaz, *Fuel*, 2007, **86**, 1216.

7 X. Dupain, E.D. Gamas, R. Madon, C.P. Kelkar, M. Makkee, J.A. Moulijn, *Fuel*, 2003, **82**, 1559.

8 I. Shimada, K. Takizawa, H. Fukunaga, N. Takahashi, T. Takatsuka, *Fuel*, 2015, **161**, 207.

9 P.J. Tancell, M.M. Rhead, R.D. Pemberton, J. Braven, *Fuel*, 1996, **75**, 717.

10 T.G. Kaufmann, A. Kaldor, G.F. Stuntz, M.C. Kerby, L.L. Ansell, *Catal. Today.*, 2000, **62**, 77.

11 N. Katada, Y. Kawaguchi, K. Takeda, T. Matsuoka, N. Uozumi, K. Kanai, S. Fujiwara, K. Kinugasa, K. Nakamura, S. Suganuma, M. Nanjo, *Appl. Catal. A Gen.* 2017, **530**, 93.

12 G. Xu, Y. Zhang, Y. Fu, Q. Guo, *ACS Catal.* 2017, **7**, 1158.

13 V. Calemma, R. Giardino, M. Ferrari, *Fuel Process. Technol.*, 2010, **91**, 770.

14 A. Gutiérrez, J.M. Arandes, P. Castaño, M. Olazar, J. Bilbao, *Fuel*, 2012, **94**, 504.

15 N. Jin, G. Wang, L. Yao, M. Hu, J. Gao, *Ind. Eng. Chem. Res.*, 2016, **55**, 5108.

16 H. Zhang, X. Zhu, X. Chen, P. Miao, C. Yang, C. Li, *Energy Fuels.*, 2017, **31**, 2749.

17 V. Nigam, S.N. Reddy, P.S.T. Sai, *Indian Chem. Eng.* 2019, **61**, 329–341.

18 J. Lee, Y. Choi, J. Shin, J.K. Lee, *Catal. Today.*, 2016, **265**, 144.

19 J. Shin, Y. Oh, Y. Choi, J. Lee, J.K. Lee, *Appl. Catal. A Gen.*, 2017, **547**, 12.

20 G.C. Laredo, P. Pérez-Romo, J. Escobar, J.L. Garcia-Gutierrez, P.M. Vega-Merino, *Ind. Eng. Chem. Res.*, 2017, **56**, 10939.

21 Y. Choi, J. Lee, J. Shin, S. Lee, D. Kim, J.K. Lee, *Appl. Catal. A Gen.*, 2015, **492**, 140.

22 X. Liu, K.J. Smith, *Appl. Catal. A Gen.*, 2008, **335**, 230.

23 M. Pang, X. Chen, Q. Xu, C. Liang, *Appl. Catal. A Gen.*, 2015, **490**, 146.

24 M. Pang, X. Wang, W. Xia, M. Muhler, C. Liang, *Ind. Eng. Chem. Res.*, 2013, **52**, 4564.

25 M. Pang, C. Liu, W. Xia, M. Muhler, C. Liang, *Green Chem.*, 2012, **14**, 1272.

26 A. Corma, V. González-Alfaro, A. V. Orchillés, *J. Catal.*, 2001, **200**, 34.

27 M. Santikunaporn, J.E. Herrera, S. Jongpatiwut, D.E. Resasco, W.E. Alvarez, E.L. Sughrue, *J. Catal.*, 2004, **228**, 100.

28 R. Bounaceur, G. Scacchi, P.M. Marquaire, F. Dominé, *Ind. Eng. Chem. Res.*, 2000, **39**, 4152.

29 A.T. Townsend, J. Abbot, *Appl. Catal. A, Gen.*, 1993, **95**, 221.

30 A. Townsend, *Appl. Catal. A Gen.*, 1992, **90**, 97.

31 M. Niwa, N. Katada, *Chem. Rec.*, 2013, **13**, 432.

32 E.P. Barrett, L.G. Joyner, P.P. Halenda, *J. Am. Chem. Soc.*, 1951, **73**, 373.

33 K. Suzuki, N. Katada, M. Niwa, *J. Phys. Chem. C.*, 2007, **111**, 894.

34 S. Suganuma, Y. Murakami, J. Ohyama, T. Torikai, K. Okumura, N. Katada, *Catal. Lett.*, 2015, **145**, 1904.

35 M. Niwa, K. Suzuki, N. Katada, T. Kanougi, T. Atoguchi, *J. Phys. Chem. B.*, 2005, **109**, 18749.

36 R. Roque-Malherbe, *Microporous Mesoporous Mater.*, 2000, **41**, 227.

37 M.A. Camblor, A. Corma, S. Valencia, *Microporous Mesoporous Mater.*, 1998, **25**, 59.

Table 1

List of applied zeolites

Notation	Framework type	Si / Al_2	Cation of the supplied form	Supplier	Product name
M15	MOR	15	Na	Catalysis Society of Japan	JRC-Z-M15
Z22	MFI	22	NH_4	Tosoh	HSZ-820NHA
Y5	FAU	5.3	Na	Catalysis Society of Japan	JRC-Z-Y5.3
B28	*BEA	28	OSDA	Tosoh	HSZ-930NHA
B25	*BEA	25	Na	Catalysis Society of Japan	JRC-Z-B25(1)
B150	*BEA	150	H	Catalysis Society of Japan	JRC-Z-HB150(1)
B500	*BEA	500	H	Tosoh	HSZ-980HOA

Table 2

Composition, textual properties and acidic properties

Notation	Al content / mol kg^{-1}	Micropore Volume / cm^3 g^{-1}		External surface area *1 / m^2 g^{-1}	Acid amount / mol kg^{-1}		ΔH *5 / kJ mol^{-1}
		[I] *1	[II] *2		BAS *3	LAS *4	
Zeolite catalysts applied in this study							
M15	1.90	0.185	0.195	33	0.95	<0.01	153
Z22	1.35	0.148	0.134	29	1.14	<0.01	139
Y5	4.23	0.339	0.314	5	1.56	0.53	116
B28	1.09	0.337	0.223	31	0.83	0.04	127
B25	1.21	0.256	0.188	102	0.36	0.02	128
B150	0.22	0.288	0.224	91	0.10	<0.01	131
B500	0.07	0.250	0.183	13	0.05	<0.01	126
Literature data							
MOR	2.32	0.169 *6	-	-	-	-	-
MFI	0.98	0.114 *6	-	-	-	-	-
FAU	4.65	0.305 *6	-	-	-	-	-
*BEA	1.23	0.155 *7	-	-	-	-	-
	0.04	0.190 *7	-	-	-	-	-

*1 calculation based on a *t*-plot method, *2 volume of condensed liquid nitrogen based on a numerical expression Ex. (1), *3 Brønsted acid sites, *4 Lewis acid sites, *5 mode value in enthalpy of ammonia desorption from Brønsted acid sites as a parameter of the acid strength, *6 Ref. [36], *7 Ref. [37].

Figure Captions

Figure 1 Schematic drawing of FCC and hydrocracking/hydrogenation of alkylaromatic hydrocarbons

Figure 2 Schematic drawing of novel process with dealkylation of alkylaromatic hydrocarbons

Figure 3 Reaction systems

Figure 4 Turnover frequency (TOF) and the products selectivities averaged between 3-5 h in tetralin conversion over various zeolites. Reaction conditions: catalyst 0.20 g, $W_{cat}/F_{reactant}$ 12 g h mol^{-1}, reaction temperature 623 K, total pressure 4 MPa. The undetectable products were carbonaceous deposited on the catalysts and gaseous compounds such as C1-4 hydrocarbons.

Figure 5 Turnover frequency (TOF) and the products selectivities averaged between 3-5 h in butylbenzene conversion over various zeolites. Reaction conditions: catalyst 0.20 g, $W_{cat}/F_{reactant}$ 12 g h mol^{-1}, reaction temperature 623 K, total pressure 4 MPa. The undetectable products were carbonaceous deposited on the catalysts and gaseous compounds such as C1-4 hydrocarbons.

Figure 6 Turnover frequency (TOF) and the products selectivities averaged between 3-5 h in indane conversion over various zeolites. Reaction conditions: catalyst 0.20 g, $W_{cat}/F_{reactant}$ 12 g h mol^{-1}, reaction temperature 623 K, total pressure 4 MPa. The undetectable products were carbonaceous deposited on the catalysts and gaseous compounds such as C1-4 hydrocarbons.

Figure 7 Influence of Brønsted acid amounts of *BEA zeolites on conversion and the products selectivities in tetralin conversion. Reaction conditions: catalyst 0.20 g, $W_{cat}/F_{reactant}$ 12 g h mol^{-1}, reaction temperature 623 K, total pressure 4 MPa. The undetectable products were carbonaceous deposited on the catalysts and gaseous compounds such as C1-4 hydrocarbons.

Figure 8 Influence of contact time ($W_{cat}/F_{reactant}$) on conversion, TOF, and the products selectivities in tetralin conversion over B28. Reaction conditions: catalyst 0.20 g, reaction temperature 623 K, total pressure 4 MPa.

Figure 9 Influence of total pressure on conversion and the products selectivities in tetralin conversion over B28. Reaction conditions: catalyst 0.20 g, $W_{cat}/F_{reactant}$ 12 g h mol^{-1}, reaction temperature 623 K.

Figure 10 Influence of reaction temperature on conversion and the products selectivities in tetralin conversion over B28. Reaction conditions: catalyst 0.20 g, $W_{cat}/F_{reactant}$ 12 g h mol^{-1}, total pressure 4 MPa.

Figure 11 Reaction pathways in conversion of tetralin. (TEX: Toluene, ethylbenzene and xylenes)

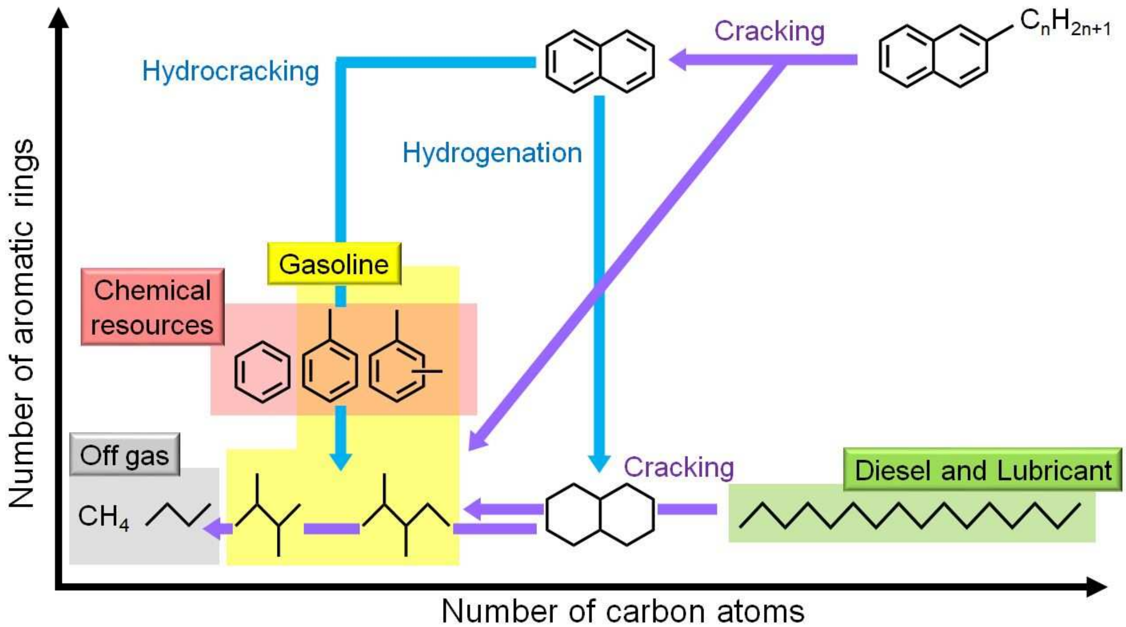
Number of aromatic rings
Number of carbon atoms
Hydrocracking
Hydrogenation
Cracking
C_nH_{2n+1}
Chemical resources
Gasoline
Off gas
CH_4
Cracking
Diesel and Lubricant

Figure 1

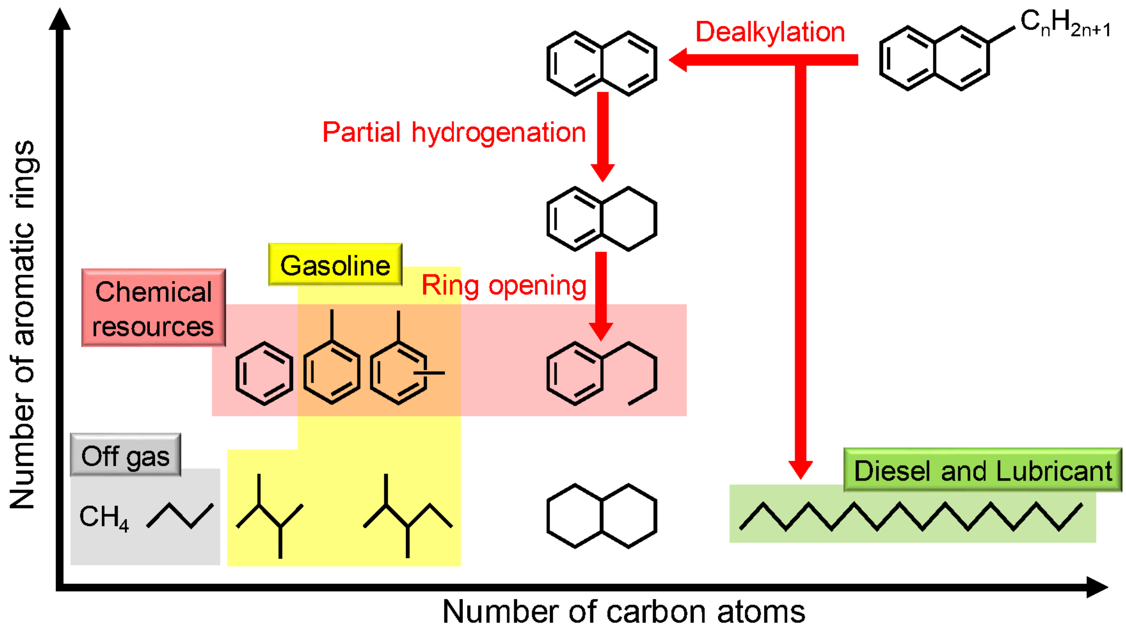
Dealkylation
C_nH_{2n+1}
Partial hydrogenation
Gasoline
Ring opening
Chemical resources
Off gas
CH_4
Diesel and Lubricant
Number of aromatic rings
Number of carbon atoms

Figure 2

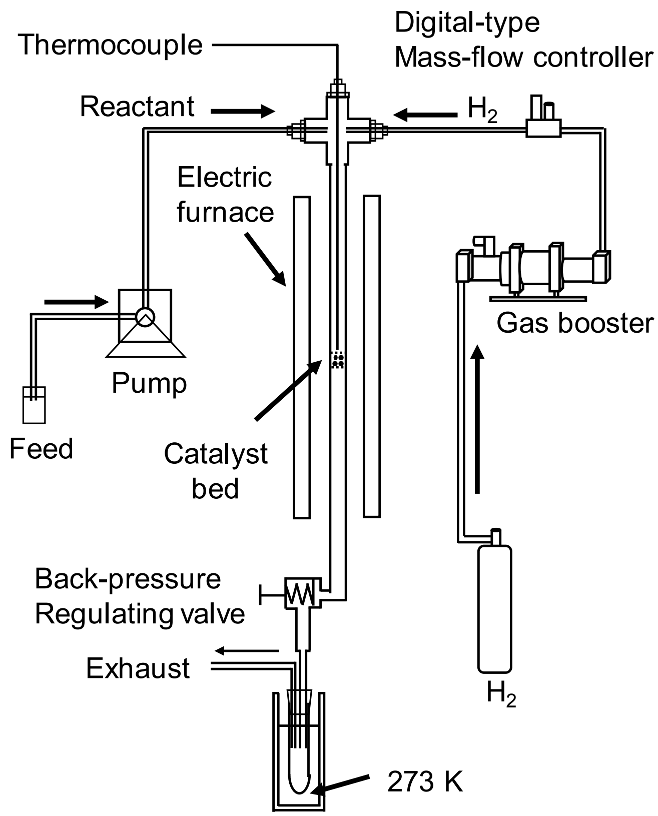
Thermocouple
Digital-type
Mass-flow controller
Reactant
H_2
Electric
furnace
Gas booster
Pump
Feed
Catalyst
bed
Back-pressure
Regulating valve
Exhaust
H_2
273 K

Figure 3

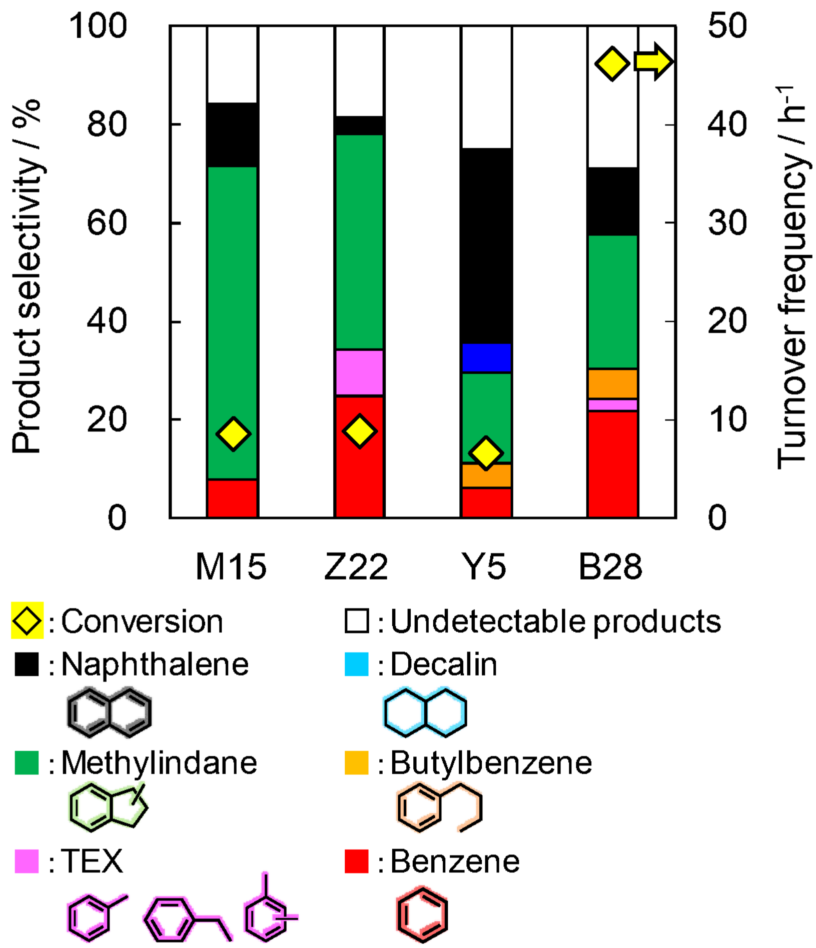
100
80
60
40
20
0
50
40
30
20
10
0
Product selectivity / %
Turnover frequency / h-1
M15
Z22
Y5
B28
: Conversion
: Undetectable products
: Naphthalene
: Decalin
: Methylindane
: Butylbenzene
: TEX
: Benzene

Figure 4

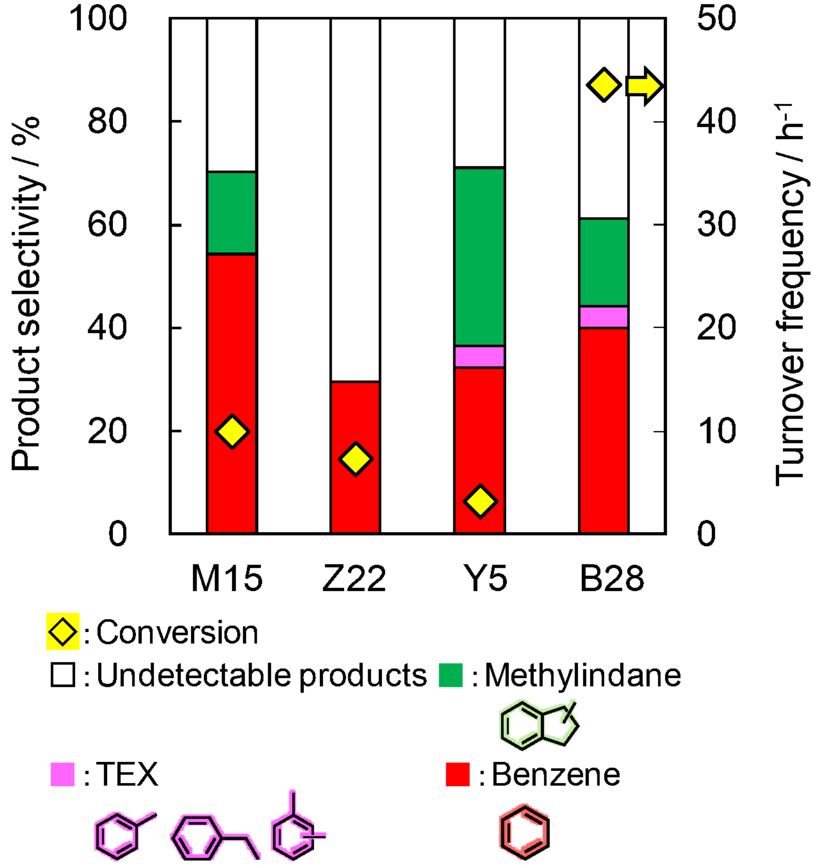
100
80
60
40
20
0
Product selectivity / %
50
40
30
20
10
0
Turnover frequency / h-1
M15
Z22
Y5
B28
: Conversion
: Undetectable products
: Methylindane
: TEX
: Benzene

Figure 5

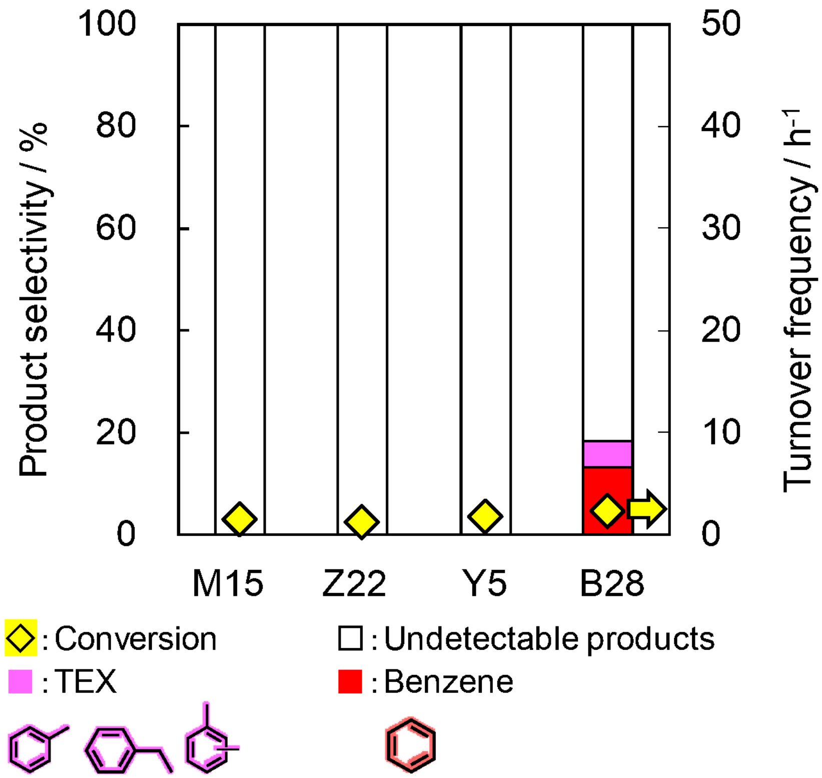
100
80
60
40
20
0
50
40
30
20
10
0
Product selectivity / %
Turnover frequency / h-1
M15
Z22
Y5
B28
: Conversion
: Undetectable products
: TEX
: Benzene

Figure 6

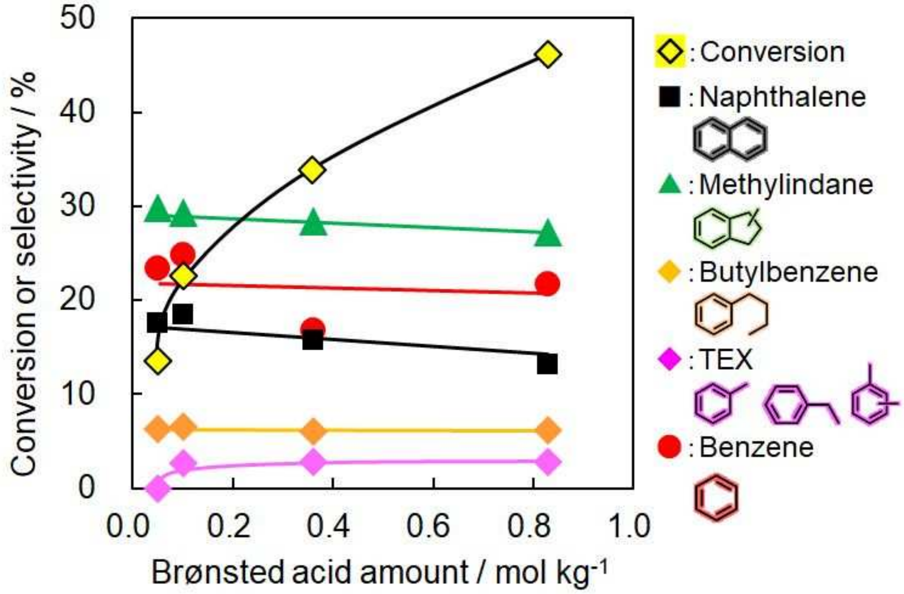
50
40
30
20
10
0
0.0
0.2
0.4
0.6
0.8
1.0
Conversion or selectivity / %
Brønsted acid amount / mol kg-1
: Conversion
: Naphthalene
: Methylindane
: Butylbenzene
: TEX
: Benzene

Figure 7

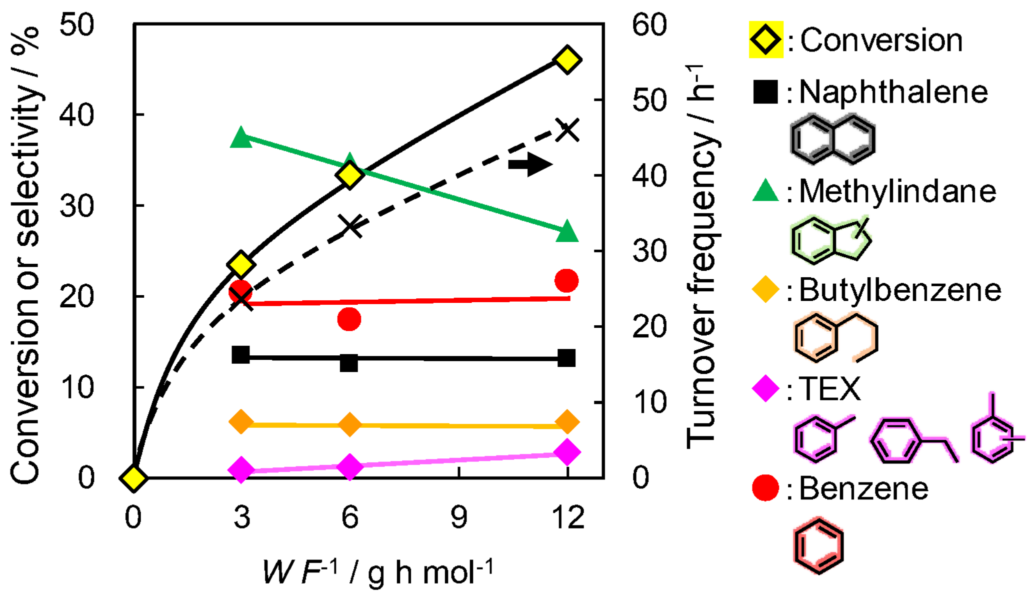
Conversion or selectivity / %
0
10
20
30
40
50
Turnover frequency / h-1
0
10
20
30
40
50
60
0
3
6
9
12
W F-1 / g h mol-1
: Conversion
: Naphthalene
: Methylindane
: Butylbenzene
: TEX
: Benzene

Figure 8

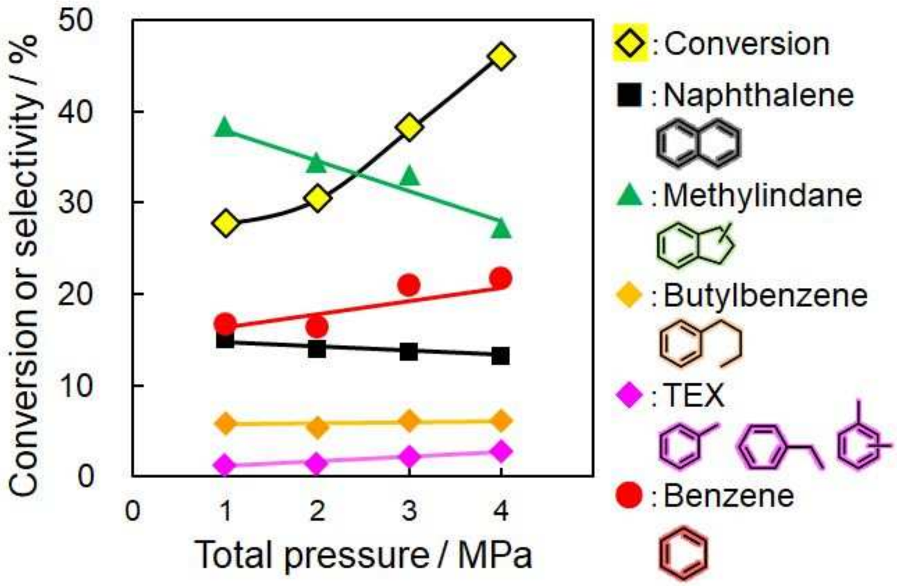
Conversion or selectivity / %
50
40
30
20
10
0
0
1
2
3
4
Total pressure / MPa
: Conversion
: Naphthalene
: Methylindane
: Butylbenzene
: TEX
: Benzene

Figure 9

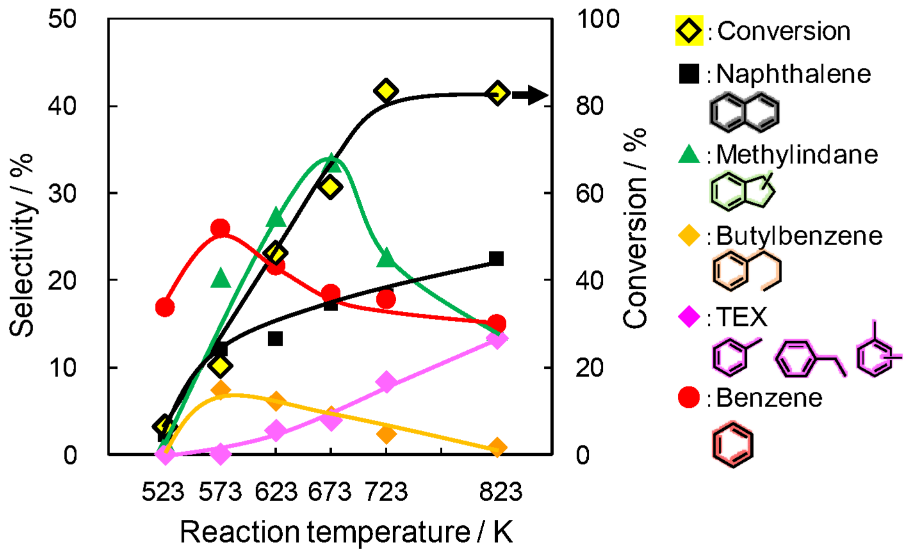

50
40
30
20
10
0
100
80
60
40
20
0
Selectivity / %
Conversion / %
523 573 623 673 723 823
Reaction temperature / K
: Conversion
: Naphthalene
: Methylindane
: Butylbenzene
: TEX
: Benzene

Figure 10

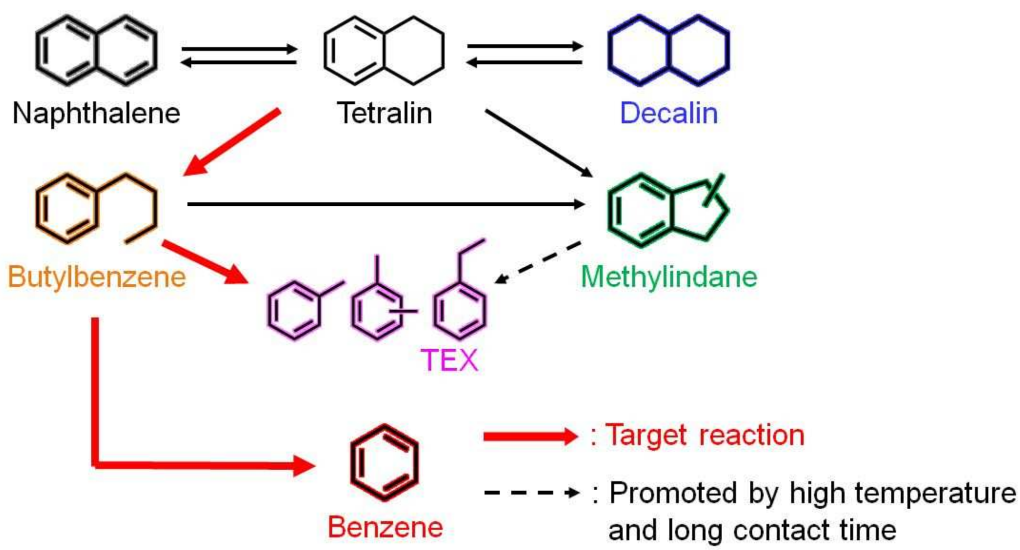
Naphthalene
Tetralin
Decalin
Butylbenzene
Methylindane
TEX
Benzene
: Target reaction
: Promoted by high temperature and long contact time

Figure 11